

# Detection of Lipid Pool, Thin Fibrous Cap, and Inflammatory Cells in Human Aortic Atherosclerotic Plaques by Near-Infrared Spectroscopy

Pedro R. Moreno, MD; Robert A. Lodder, PhD; K. Raman Purushothaman, MD; William E. Charash, MD, PhD; William N. O'Connor, MD; James E. Muller, MD

**Background**—A method is needed to identify nonstenotic, lipid-rich coronary plaques that are likely to cause acute coronary events. Near-infrared (NIR) spectroscopy can provide information on the chemical composition of tissue. We tested the hypothesis that NIR spectroscopy can identify plaque composition and features associated with plaque vulnerability in human aortic atherosclerotic plaques obtained at the time of autopsy.

**Methods and Results**—A total of 199 samples from 5 human aortic specimens were analyzed by NIR spectroscopy. Features of plaque vulnerability were defined by histology as presence of lipid pool, thin fibrous cap ( $<65 \mu\text{m}$  by ocular micrometry), and inflammatory cell infiltration. An InfraAlyzer 500 spectrophotometer was used. Spectral absorbance values were obtained as log (1/R) data from 1100 to 2200 nm at 10-nm intervals. Principal component regression was used for analysis. An algorithm was constructed with 50% of the samples used as a reference set; blinded predictions of plaque composition were then performed on the remaining samples. NIR spectroscopy sensitivity and specificity for histological features of plaque vulnerability were 90% and 93% for lipid pool, 77% and 93% for thin cap, and 84% and 89% for inflammatory cells, respectively.

**Conclusions**—NIR spectroscopy can identify plaque composition and features associated with plaque vulnerability in postmortem human aortic specimens. These results support efforts to develop an NIR spectroscopy catheter system to detect vulnerable coronary plaques in living patients. (*Circulation*. 2002;105:923-927.)

**Key Words:** atherosclerosis ■ plaque ■ tissue ■ spectroscopy

There is widespread agreement that new diagnostic techniques are required to identify coronary plaques that are prone to disruption.<sup>1-3</sup> The type of plaque considered to be most vulnerable to disruption is a thin-capped fibroatheroma with increased inflammatory cell content.<sup>4-6</sup> Multiple techniques are being tested to identify such plaques before they disrupt and cause thrombosis.<sup>7-14</sup> Identification of these potentially lethal plaques before they disrupt will facilitate the development of therapeutic strategies to prevent acute coronary events.

Diffuse reflectance near-infrared (NIR) spectroscopy has been used extensively to identify the chemical content of biological specimens.<sup>15</sup> NIR spectroscopy is based on the absorbance of light by organic molecules. The reflectance spectra from wavelengths between 400 and 2400 nm allow detailed analysis of chemical composition. NIR can provide simultaneous, multicomponent, non-destructive chemical analysis of biological tissue with acquisition time  $<1$  second.<sup>15</sup> No sample preparation is required, and physical and biological properties as well as molecular information can be derived from spectra. NIR spectroscopy has been used to monitor

systemic and cerebral oxygenation and to identify hundreds of plasma constituents including glucose, total protein, triglycerides, cholesterol, urea, creatinine, and uric acid.<sup>16-20</sup> NIR can also characterize human metalloproteins.<sup>21</sup>

Our group has reported on the use of NIR spectroscopy to identify cholesterol, HDL, and LDL in arterial wall samples.<sup>22,23</sup> Images of fibrous cap, lipids, thrombus, ulceration, and necrosis found in carotid endarterectomy specimens from humans have also been obtained with the use of a focal plane array NIR video camera.<sup>23</sup>

The present study was designed to test the hypothesis that NIR spectroscopy can identify plaque composition and features associated with vulnerability in human aortic atherosclerotic plaques obtained at the time of autopsy.

## Methods

### Histological Analysis

Five explanted human aortas were obtained at the time of postmortem analysis. From each aorta, aortic wall circumferential strips

Received September 27, 2001; revision received December 11, 2001; accepted December 21, 2001.

From The Linda and Jack Gill Heart Institute, University of Kentucky (P.R.M., R.A.L., K.R.P., W.N.O.), Lexington; the Department of Surgery (W.E.C.), Boston University School of Medicine; the Cardiac Unit (J.E.M.), Massachusetts General Hospital, Harvard Medical School, Boston; and InfraReDx, Cambridge, Mass.

Drs Moreno, Lodder, Charash, O'Connor, and Muller are cofounders and active shareholders of InfraReDx. Dr Purushothaman is an active shareholder of InfraReDx. Correspondence to Pedro R. Moreno, MD, 111B-CDD, Veterans Administration Medical Center, 2250 Leestown Road, Lexington, KY 40511. E-mail pmoreno@uky.edu

© 2002 American Heart Association, Inc.

*Circulation* is available at <http://www.circulationaha.org>

DOI: 10.1161/hc0802.104291

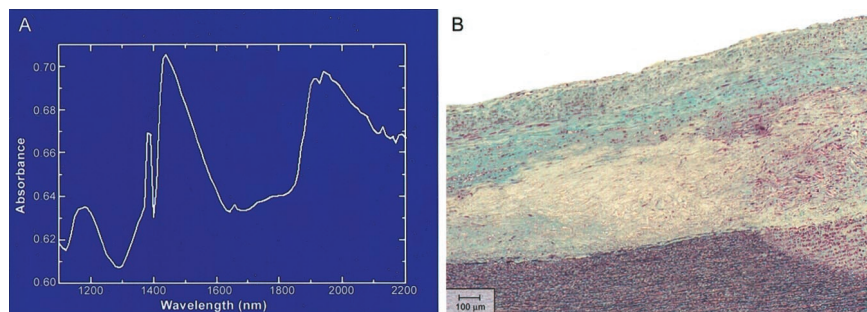


**Figure 1.** NIR spectra collected from atherosclerotic, lipid-rich aortic plaque. A, NIR absorbance tracing from spectra collected with an InfraAlyzer 500 spectrophotometer. Absorbance values were collected from 1100- to 2200-nm wavelength window at 10-nm intervals (see text for details). B, Lipid-rich aortic plaque (elastic trichrome staining).

(55 mm in length and 10 mm in width) were obtained above the origin of the celiac trunk. Each strip was fixed in 10% buffered formalin and sequentially cut into tissue segments measuring  $1.5 \times 10$  mm, with a total area of 15 mm<sup>2</sup> per segment. Segments were all scanned sequentially. A total of 248 segments were prepared. After NIR scanning, each segment was imbedded in paraffin and processed by conventional techniques. Serial 5- $\mu$ m sections were cut from each segment until the halfway point of  $\approx 750$   $\mu$ m was reached. Subsequently, the next two sequential 5- $\mu$ m-thick sections were selected from each segment, mounted on lysine-coated slides, and stained by hematoxylin and eosin and by a modification of the elastic tissue–Masson’s trichrome method developed by one of the authors and now in widespread use for evaluation of vascular structures.<sup>24</sup> Each section was evaluated by light microscopy by two experienced pathologists for the presence or absence of lipid pool, thin fibrous cap, and inflammatory cells. After processing, lipid appeared as predominately solvent-treated empty spaces in stained sections. We defined lipid pool as morphologically distinct spaces composed of clear, needle-shaped cholesterol clefts (representing ghost outlines of dissolved crystals) and/or clear, bubbly, granular, mostly anucleate necrotic debris of foam cells. Lipid pool area was determined by computerized planimetry as previously reported.<sup>25</sup> Mean ( $\pm$ SD) lipid pool area was  $5.3 \pm 3.2$  mm<sup>2</sup> and ranged from 1.00 to 16.36 mm<sup>2</sup>. Thus, the cutoff point for considering a segment positive for lipid was set at the minimum measured area of 1.00 mm<sup>2</sup>. Thin fibrous cap was defined as a cap thickness of  $\leq 65$   $\mu$ m,<sup>26</sup> determined with the use of an ocular micrometer. The device was calibrated in the reticle (Olympus WK 10x/20L) to a minimal interval of 2  $\mu$ m with the use of an Olympus DplanApo  $\times 60$  magnification (high dry) objective. Inflammation was defined as the presence of  $\geq 25$  mononuclear round cells per field in hematoxylin and eosin-stained sections with the  $\times 40$  magnification objective.<sup>26</sup> Pathologists were blinded to the results of the NIR analysis.

### NIR Spectroscopic Analysis

After cutting, each aortic segment (with a total area of 15 mm<sup>2</sup>) was placed on a 5 $\times$ 5-cm alumina platform neutral to NIR light. A NIR probe with a scanning area of 78 mm<sup>2</sup> was aligned over each segment and lowered until it was in contact with the tissue. Hence, the entire segment contributed to the NIR signal. The specimen was not immersed in water or blood during the measurement. The acquisition time for a single scan was 2 minutes.

### Instrumentation

The study was conducted with an InfraAlyzer 500 (Bran and Luebbe) spectrophotometer. The instrument uses a tungsten light source to generate near-infrared light, with a maximum power of 300 mW, which provides tissue penetration of  $\approx 2$  mm. Absorbance values were obtained as  $\log(1/R)$  data from 1100 to 2200 nm at 10-nm intervals (Figure 1). Analytical software was written in Mathematica 3.0 (Wolfram Research, Inc), Matlab 5.1 (The Math Works, Inc), and Speakeasy IV Eta (Speakeasy Computing Corp). Calibration was performed with the use of the Caldatas program.<sup>27</sup> Three NIR scans were performed on each segment. Principal component regression was used to analyze the smoothed, scatter-corrected data. This regression technique transforms a large number of correlated variables into a new set of noncorrelated variables, reducing the

dimensionality of a data set by linear transformation with principal components (PCs). The PCs are structured so that the first few retain most of the variation contained in all the original variables. Thus, the first PC contains information from the constituent, which contributes most to the total NIR spectral variation of the data. The second PC is orthogonal to the first and weighs most heavily the wavelengths that contribute most to the variation of the spectra after removal of the first PC. Progressively smaller contributions to the spectral variation are described by additional orthogonal PCs. A total of four PCs was used for the analysis.

### Algorithm Development and Statistical Analysis

Histology was used as the gold standard to validate NIR spectroscopy results. The NIR spectra obtained from 50% of the samples (the training set) were used to develop an algorithm to classify the samples for presence or absence of lipid pool, thin fibrous cap, and increased inflammatory cell infiltration. The algorithm was then tested for its ability to predict plaque composition on unknown samples (the test set). Spectra associated with each of the three histological features of interest were defined by the results of the training set. Thus, samples rich in lipid produced one type of spectra, those with thin caps produced another, and samples with inflammatory infiltrates produced a third. In each case, the spectra merely represent the chemicals associated with the histological finding. For instance, in cases of inflammation, it is likely that certain chemicals are found in higher concentration than in noninflamed plaques.<sup>23</sup> In the present study, major spectral features correlating with inflammation were observed at 1300, 1600, and 2100 nm.

NIR spectra were correlated to the histology, as previously described.<sup>22,23</sup> Cross validation was used on the entire group of samples, and calibration was performed by the bootstrap error-adjusted, single-sample technique<sup>22</sup> before blinded prediction of the test set. Sensitivity, specificity, and positive and negative predictive values were calculated by the use of established formulas. Total time for data analysis was  $\approx 4$  CPU hours on a 400-MHz PII computer.

### Results

A total of 248 segments were analyzed by NIR spectroscopy and by histology. A total of 49 specimens were excluded. Of these, 42 were excluded for histological problems including missing intima (34), broken fibrous cap (4), section artifact (3), and intercostal branch (1). Seven additional samples were excluded because of technical inadequacies of the NIR signal, leaving a total of 199 specimens in the study. One hundred samples were used as a training set to develop an algorithm to classify the samples for presence or absence of lipid pool, thin fibrous cap, and increased inflammatory cell infiltration. Both training and test sets contained samples randomly chosen from all 5 autopsy specimens.

The NIR spectra from the training set were identified as belonging to plaques with the histological features of interest. From this information, the computer, through the use of PC algorithms, learned the types of spectra associated with

**TABLE 1. Detection of Plaque Composition by NIR Spectroscopy and Histology**

	Histology						
	Lipid Pool		Thin Cap		Inflammation		
	+	-	+	-	+	-	
NIR Spectroscopy	+	35	4	13	6	37	6
	-	4	56	4	76	7	49

different types of plaques. The remaining 99 samples were used to test the prediction of plaque composition. In working with the test set, the spectroscopist was blinded to the histological characteristics of the sample.

Results are given in Table 1. NIR spectroscopy identified 35 of 39 lesions (90%) with lipid pool and 56 of 60 lesions (93%) without lipid pool (Figure 2, A and B). For fibrous cap thickness, NIR identified 13 of 17 lesions (77%) with thin cap and 76 of 82 lesions (93%) with thick cap (Figure 2, C and D). Finally, NIR identified 37 of 44 lesions (84%) with inflammatory cells and 49 of 55 lesions (89%) without inflammatory cells (Figure 2, E and F). Sensitivity and specificity for the various characteristics are shown in Table 2.

**Discussion**

This blinded, controlled study indicates that NIR spectroscopy can identify histological features of vulnerability in

**TABLE 2. NIR Detection of Plaque Composition Determined by Histology**

	Lipid Pool	Thin Cap	Inflammation
Sensitivity	90	77	84
Specificity	93	93	89
Positive predictive value	90	68	86
Negative predictive value	93	95	88

human aortic plaques obtained at autopsy. The technique achieved 90% sensitivity and 93% specificity for identification of lipid-rich atherosclerotic plaques characteristic of those commonly associated with acute ischemic events.<sup>1-6</sup> In addition, the sensitivity and specificity for identification of thin fibrous caps and inflammatory cells ranged from 77% to 93%.

These findings are consistent with results obtained with NIR spectroscopy by other investigators. Jarros et al<sup>20</sup> determined cholesterol content of human aortic plaques obtained at autopsy by using a Fourier Transform (FT) spectrophotometer and fiberoptic systems. The correlation coefficient between cholesterol contents determined by NIR spectroscopy and by reverse-phase, high-pressure liquid chromatography was 0.96.<sup>20</sup> The study by Jarros et al used chemical content as a gold standard, whereas our study used a histological gold standard. The studies are complementary and mutually supportive.

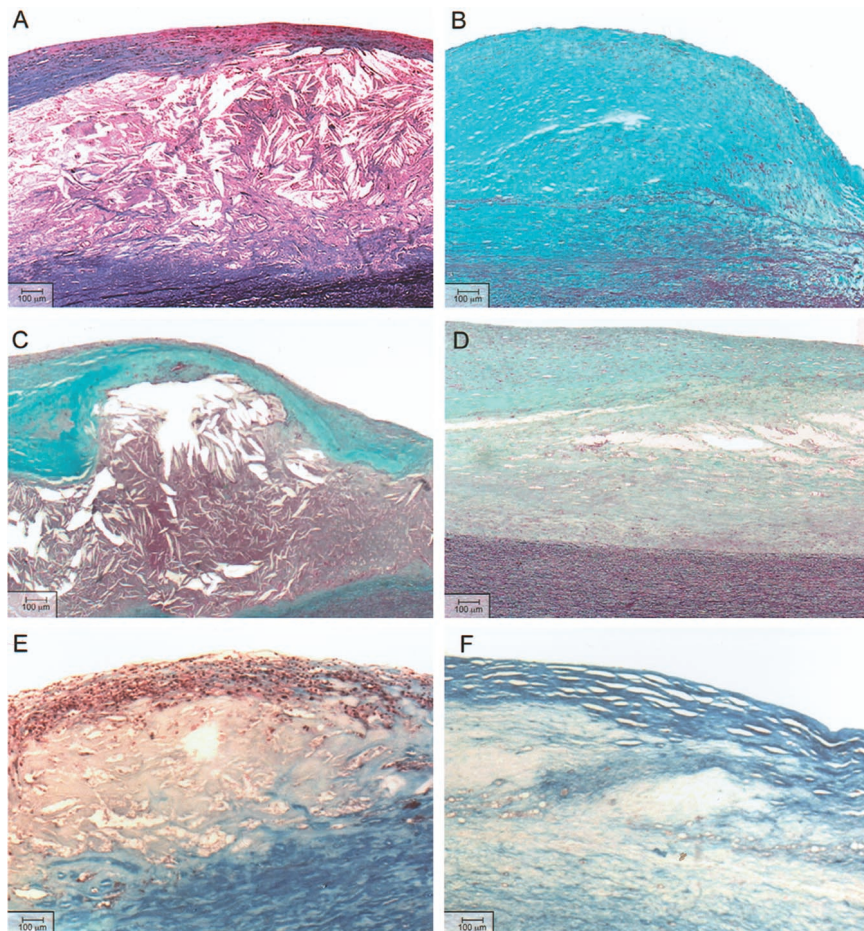


**Figure 2.** Histological examples of different microanatomic features associated with plaque vulnerability. All samples are stained by elastic trichrome method. Color of connective tissue varies, depending on ratio of collagen to elastin and other variables. Connective tissue stains blue in A, E, and F and green in B, C, and D. Macrophages stain brown in E. A, Lipid-rich plaque; B, fibrotic plaque; C, thin fibrous cap; D, thick fibrous cap; E, plaque with abundant inflammatory cells in the cap; and F, plaque without inflammatory cells.

The power of NIR spectroscopy to identify the chemical composition of biological samples is based on interactions between organic molecules and photon absorption that varies depending on the wavelength of the incident NIR light. Unique combinations of carbon-hydrogen, carbon-oxygen, and other bonds result in characteristic absorbance at specific wavelengths that can be used for sample identification. Because lipid-rich and non-lipid-rich samples contain many similar constituents (including water, which absorbs strongly in these wavelengths), the gross appearance of reflectance spectra is similar for most samples. Precise identification of subtle chemical differences is achieved through a highly developed mathematical method (principal component analysis) that compares the characteristics of equations describing the reflectance spectra. Just as the surface ECG does not reflect the electrical activity of a single myocardial cell, the reflection from a sample does not result from a single chemical component. Both signals represent a composite pattern with contributions from multiple sources. In the spectroscopic determinations, a training set is used to teach the computer the patterns associated with lipid-rich and non-lipid-rich plaques.

The importance of the NIR/histology correlation demonstrated in the study is enhanced by the current lack of a technique to identify vulnerable coronary artery plaques in living patients. Stress testing methods and coronary angiography are designed to identify stenosis. However, nonstenotic plaques are responsible for the majority of acute coronary events. Noninvasive methods such as MRI and CT have considerable potential for eventual use in the detection of vulnerable plaques.<sup>8,9</sup> However, it is likely that the noninvasive test would be used as a screening test to identify high-risk individuals who would then undergo definitive testing with an intracoronary device.

Several intracoronary methods have received attention for the detection of vulnerable plaque. Although intravascular ultrasound is an excellent method to assess stenosis and vessel wall remodeling,<sup>28</sup> its ability to identify plaque composition is limited.<sup>29</sup> Angioscopy may identify glistening yellow plaques with increased subsequent coronary events. However, the technique requires coronary occlusion.<sup>11</sup> Thermography is based on the novel observation that plaques with inflammation are warmer than control plaques.<sup>12</sup> In vivo studies have demonstrated increased temperature in plaques from patients with acute coronary events,<sup>13</sup> supporting the hypothesis that nondisrupted vulnerable plaques may be detected by identification of a temperature gradient. Optical coherence tomography obtains images based on reflection of light with an exceptional resolution of 10  $\mu\text{m}$ .<sup>10</sup> However, it cannot obtain images through blood. Other techniques such as intravascular MRI and Raman spectroscopy are under intense investigation for human implementation.<sup>7,8,14</sup>

An important feature of the present in vitro study is the high likelihood that the method can be adapted for coronary plaque characterization in living patients. Of foremost importance is that NIR light can be safely delivered to the human coronary by a fiberoptic catheter. In the present correlation study, the light was supplied by a tungsten source and ranged from 1100 to 2200 nm in wavelength. For a study in patients,

it is likely that a smaller number of wavelengths can be identified that is sufficient for vulnerable plaque identification. For such clinical studies, in which a minimum exposure to light and maximum speed of data acquisition are desirable, it is likely that a laser delivering light in a small number of informative wavelengths will be the optimal light source.

For use in the human coronary artery, it is desirable that the measurement be made through blood, without the need for direct contact with the arterial wall, thereby eliminating the need for flushing or occlusion of the coronary artery. There are both theoretical reasons and experimental data supporting the possibility that NIR spectroscopy can be performed through blood, without tissue contact. With regard to the theoretical issue, cholesterol and other compounds of interest have strong absorbance peaks in the range from 1600 to 1800 nm. Whereas water and blood absorb heavily around a broad peak at 1500 nm and after 1800 nm,<sup>30,31</sup> a cholesterol peak occurs at 1700 to 1800 nm in an area of relatively decreased water absorbance, sometimes referred to as a "water window." The method described in this report relies on the ability of principal component analysis to isolate the critical data describing lipid absorbance from the strong signals indicating absorbance by water. With regard to experimental data, in a prior study, a member of our group (with others) demonstrated that NIR spectroscopy can identify cholesterol, HDL, and LDL in living arterial tissue through blood, without direct contact with the vessel wall.<sup>22</sup>

### Limitations

The internal validity of this correlation study is limited by a discrepancy between the source of the NIR signal (the gross tissue segment) and the source of the histological information (two adjacent 5- $\mu\text{m}$  sections from the center of each segment). If the variation caused by this discrepancy were diminished by more frequent histological sampling, the correlations would be even higher than those observed. Future studies, which will greatly increase the volume of data available, will provide answers required before clinical utility is achieved.

This study is limited to the variability observed in the aortas of 5 patients. Additional studies are required to increase the knowledge of the variability likely to be encountered in an unknown subject. In this study, there was no attempt to differentiate a necrotic core from a lipid pool. Because these structures may cause different risks of disruption, future studies based on histological stains that can differentiate the two are needed. The spectroscopic signal, which is determined by chemical content, is expected to be different in areas rich in free versus esterified cholesterol. Studies are also needed of the NIR features of ruptured plaques and those with internal hemorrhage, because such plaques will be encountered in patients for whom the technique is intended.

It is likely that the combination of indexes of intimal thickness, lipid content, and presence of inflammatory cells will have a greater predictive value for a clinical event than any single index. Although the present study was sufficient to demonstrate the ability of NIR spectroscopy to identify correlations for individual indexes, subsequent studies with

larger numbers of samples and increased statistical power are required to test the correlations for identification of multiple plaque features.

### Future Studies

The positive result obtained in the present study supports the conduct of subsequent studies to answer questions that must be addressed before the introduction of a technique that will be useful for the care of patients. Spectroscopic information is dependent on a range of variables including temperature, pH, and breakdown of tissue.<sup>7</sup> Hence, this promising in vitro ability of NIR spectroscopy to detect signs associated with vulnerability must be tested in vivo in an animal model and in living patients. Furthermore, validation of these results in coronary plaques is also needed. The current system was used to establish proof-of-principle without regard for speed of data acquisition or processing. There is no obstacle to construction of a system that will function much faster. Acquisition and processing speeds similar to those of intravascular ultrasound can be achieved, which will permit scanning of the coronary vessels in a timely manner.

### Conclusions

NIR spectroscopy successfully identified components of plaque vulnerability (thin cap, lipid pool, and macrophage presence) in postmortem specimens from human atherosclerotic plaques. These results support efforts to develop an NIR catheter system for use in the coronary arteries of living patients. Such an NIR system, probably in combination with other intracoronary diagnostic modalities, would facilitate the conduct of randomized studies of plaque stabilization to prevent the acute coronary syndromes.

### Acknowledgments

This study was supported in part by a research grant to Dr Pedro R. Moreno from InfraReDx, Inc, a private company that is developing NIR spectroscopy for detection of vulnerable plaque in patients. We thank Drs Valeri Vyalkov and Eric Ryan for help in data collection and analysis.

### References

- Falk E, Shah PK, Fuster V. Coronary plaque disruption. *Circulation*. 1995;92:657–671.
- Davies MJ. Detecting vulnerable coronary plaques. *Lancet*. 1996;347:1422–1423.
- Muller JE, Abela GS, Nesto RW, et al. Triggers, acute risk factors and vulnerable plaques: the lexicon of a new frontier. *J Am Coll Cardiol*. 1994;23:809–813.
- Virmani R, Kolodgie FD, Burke AP, et al. Lessons from sudden coronary death: a comprehensive morphological classification scheme for atherosclerotic lesions. *Arterioscler Thromb Vasc Biol*. 2000;20:1262–1275.
- Buja LM, Willerson JT. Role of inflammation in coronary plaque disruption. *Circulation*. 1994;89:503–505.
- Libby P. Molecular basis of the acute coronary syndromes. *Circulation*. 1995;91:2844–2850.
- Naghavi M, Madjid M, Khan MR, et al. New developments in the detection of vulnerable plaque. *Curr Atheroscler Rep*. 2001;3:125–135.
- Pasterkamp G, Falk E, Woutman H, et al. Techniques characterizing the coronary atherosclerotic plaque: influence on clinical decision making? *J Am Coll Cardiol*. 2000;36:13–21.
- Fayad ZA, Fuster V. Characterization of atherosclerotic plaques by magnetic resonance imaging. *Ann N Y Acad Sci*. 2000;902:173–186.
- Brezinski ME, Tearney GJ, Weissman NJ, et al. Assessing atherosclerotic plaque morphology: comparison of optical coherence tomography and high frequency intravascular ultrasound. *Heart*. 1997;77:397–403.
- Uchida Y, Nakamura F, Tomaru T, et al. Prediction of acute coronary syndromes by percutaneous coronary angiography in patients with stable angina. *Am Heart J*. 1995;130:195–203.
- Casscells W, Hathorn B, David M, et al. Thermal detection of cellular infiltrates in living atherosclerotic plaques: possible implications for plaque rupture and thrombosis. *Lancet*. 1996;347:1447–1451.
- Stefanadis C, Diamantopoulos L, Vlachopoulos C, et al. Thermal heterogeneity within human atherosclerotic coronary arteries detected in vivo: a new method of detection by application of a special thermography catheter. *Circulation*. 1999;99:1965–1971.
- Romer TJ, Brennan JF III, Puppels GJ, et al. Intravascular ultrasound combined with Raman spectroscopy to localize and quantify cholesterol and calcium salts in atherosclerotic coronary arteries. *Arterioscler Thromb Vasc Biol*. 2000;20:478–483.
- Dempsey RJ, Davis DG, Buice RG, et al. Biological and medical applications of near-infrared spectroscopy. *Applied Spectroscopy*. 1996;50:18A–34A.
- McKinley BA, Marvin RG, Cocanour CS, et al. Tissue hemoglobin O<sub>2</sub> saturation during resuscitation of traumatic shock monitored using near infrared spectrometry. *J Trauma*. 2000;48:637–642.
- Spielman AJ, Zhang G, Yang C, et al. Intracerebral hemodynamics probed by near infrared spectroscopy in the transition between wakefulness and sleep. *Brain Res*. 2000;866:313–325.
- Gabriely I, Wozniak R, Mevorach M, et al. Transcutaneous glucose measurement using near-infrared spectroscopy during hypoglycemia. *Diabetes Care*. 1999;12:2026–2032.
- Shaw RA, Kotowich S, Leroux M, et al. Multianalyte serum analysis using mid-infrared spectroscopy. *Ann Clin Biochem*. 1998;35:624–632.
- Jarros W, Neumeister V, Latke P, et al. Determination of cholesterol in atherosclerotic plaques using near infrared diffuse reflection spectroscopy. *Atherosclerosis*. 1999;147:327–337.
- Shaw RA, Mansfield JR, Kupriyanov VV, et al. In vivo optical/near-infrared spectroscopy and imaging of metalloproteins. *J Inorg Biochem*. 2000;79:285–293.
- Cassis LA, Lodder RA. Near-IR imaging of atheromas in living arterial tissue. *Anal Chem*. 1993;65:1247–1256.
- Dempsey RJ, Cassis LA, Davis DG, et al. Near-infrared imaging and spectroscopy in stroke research: lipoprotein distribution and disease. *Ann N Y Acad Sci*. 1997;820:149–169.
- O'Connor WN, Valle S. A combination of Verhoeff's elastic and Masson's trichrome stain for routine histology. *Stain Technology*. 1982;57:207–210.
- Moreno PR, Bernardi VH, Lopez-Cuellar J, et al. Macrophages, smooth muscle cells and tissue factor in unstable angina: implications for cell-mediated thrombogenicity in acute coronary syndromes. *Circulation*. 1996;94:3090–3097.
- Burke AP, Farb A, Malcom GT, et al. Coronary risk factors and plaque morphology in men with coronary disease who died suddenly. *N Engl J Med*. 1997;336:1276–1282.
- Workman J Jr. Spectroscopy calibration basics. In: Burns DA, Circzak EW eds. *Handbook of Near-Infrared Analysis*. 2nd ed. New York, NY: Marcel Dekker; 2001.
- Schoenhagen P, Ziada KM, Kapadia SR, et al. Extent and direction of arterial remodeling in stable versus unstable coronary syndromes: an intravascular ultrasound study. *Circulation*. 2000;101:598–603.
- Peters RJG, Kok WEM, Havenith MG, et al. Histopathologic validation of intracoronary ultrasound imaging. *J Am Soc Echocardiogr*. 1994;7:230–241.
- Parsa P, Jacques SL, Nishioka NS. Optical properties of rat liver between 350 and 2200 nm. *Applied Optics*. 1989;28:2325–2330.
- Brezinski M, Saunders K, Jesser C, et al. Index matching to improve optical tomography imaging through blood. *Circulation*. 2001;103:1999–2003.